

CFD Prediction of High Viscosity Oil-Water (Water-Assist) Flow Behavior in Horizontal Pipe

Solomon O. Alagbe

Abstract— The advent of high viscosity oil requires more investigations to enhance good design of transportation system and forestall its inherent production difficulties. Experimental and numerical studies were conducted on oil-water in 1-in ID 5m long horizontal perspex pipe. The densities of CYL680 and CYL1000 oils employed are 917 and 916.2kg/m³ while their viscosities are 1.830 and 3.149Pa.s at 25°C, respectively. The high viscosity oil-water interfacial tension is 0.026 N/m at 19°C. The oil superficial velocity ranged from 0.1 to 0.55m/s and water ranged from 0.2 to 1.0m/s. A three-dimensional high viscosity oil-water, two-phase co-current CFD model was developed for predicting the local hydrodynamics of flow. The transient model based on Volume of Fluid (VOF) method, considering surface tension was employed. Co-current water flow model compared favourably with the experiment. The pressure gradients decreased by 5 to 8 order of magnitude. The flow patterns, Water Assist- Annular (WA-ANN), Dispersed Oil in Water (DOW/OF), Oil Plug in Water (OPW/OF) with oil film on the wall and Water Plug in Oil (WPO), were also identified from the contour plots of the flow configurations, the trend plot, Probability Density Function (PDF) and statistical moments of the downstream pressure signalled.

Index Terms Core annular flow, Computational Fluid Dynamics (CFD), co-current flow, Probability Density Function (PDF), Water-Assisted (WA) flow.

1. INTRODUCTION

THIS Cold Heavy Oil Production (CHOP) was proposed to be an effective production method for heavy (high viscosity) oils that are located in unconsolidated reservoirs [1, 2]. Several researchers like Besson [3] and Owen *et al.* [4] reported that transportation of heavy oil is energy intensive and that the technology of pipe wall lubrication with light oils or water would reduce the energy consumption in production. A good understanding of this phenomenon is required for its smooth operation. Although some research has been done on oil flows to describe their behaviour; the flow pattern, phase hold up, pressure drop along horizontal, vertical and inclined planes (Barnea *et al.*, [5]; Martinez *et al.*, [6]; Brauner and Moalem Maron, [7]; Trallero *et al.*, [8]; Angeli and Hewitt [9,10]). However, the focus has been on low and medium viscosity oils (<1000cP), known as conventional oil. These findings cannot be relied upon for the generality of fluids because of the difference in properties, most importantly, the viscosity.

In the theoretical approach, Ooms and Poesio [11] developed a model based on lubrication theory to predict the stability of core annular flow that was adjudged inexpensive and profitable method of production. Rodriguez and Bannwart [12] proposed a stability model using an Inviscid Kelvin-Helmholtz (IKH) which provides a stability criterion that depends on Eotvos number. Kaushik [13] numerically investigated the effect of sudden contraction and expansion pipe and concluded that fouling can be minimised through such configuration. Bai [14] identified a bamboo wave pattern in upward flow as a result of buoyancy of oil which makes it lighter and therefore stretched while in the downward flow, the oil is compressed and formed corkscrew waves. This is different from the existing patterns in horizontal flows.

A number of studies have been reported on the Com-

putational Fluid Dynamics (CFD) study of liquid-liquid slug in capillary micro-structured reactor (pipe) (Kashid *et al.*, [15; 16; 17; 18; 19, 20]). The authors explored the applicability of Volume of Fluid (VOF) methodology in CFD to predict the liquid slug generation, internal circulation within slug body, flow pattern details and its hydrodynamics in a microchannel. Ghosh [21] studied the core annular flow in a vertical downward direction using CFD to generate the profiles of velocity, pressure, volume fraction and wall shear stress over a wide range of inlet oil and water velocities. This study found that an abrupt change in the radial velocity gradient occurred at the interface and that change became more prominent as flow propagates towards the outlet. The increase in both the frictional pressure gradient and wall shear stress as the superficial velocities of oil and water increase was also reported. None of the numerical research on oil-water flow in pipes, to the knowledge of the author, has been reported on the behaviours of high viscosity oil based multiphase flow in horizontal pipes.

In the literatures, different inlet design were experimentally adopted by the researchers to study the oil-water annular flow (Sotgia *et al.*, [22]; Prada and Bannwart, [23]; Bensakhria *et al.*, [24]; Balakhrisna *et al.*, [25]; Strazza *et al.*, [26]). This approach was attempted to impose the core annular flow behaviour, but has not been considered in the CFD modelling. Mathematical models are widely used in petroleum industry to predict multiphase flow behaviours. However, these models have been developed and validated based on data gathered from low-viscosity oil due to the limited experimental data for high viscosity multiphase flow. The usage of CFD for modelling multiphase flows has been gaining ground in the past two decades and the formulations of constitutive models for multiphase flows are attracting attentions of the researchers. This is due to the complex phenomena of fluid-particle, fluid-fluid, particle-particle and particle-wall interactions. In spite of the current capabilities of CFD in investigating multiphase flows, experimental data are still very useful

• Solomon O. Alagbe is currently a lecturer in the Department of Chemical Engineering at Ladoko Akintola University of Technology, Nigeria. E-mail: soalagbe@lautech.edu.ng

and needed for the verification and validation of any numerical model or simulation.

However, progress should be made in order to produce a truly predictive computational scheme, and reduce fluid flows (especially complex turbulent flows) to computable phenomena (Abdullah, [27]). Since the use of full governing Navier-Stokes equations is normally computationally impractical for the prediction of turbulent flows, a hierarchy of turbulence models is used to model fluctuations inherent in these equations. In the light of this, closure models are needed and being developed based on certain assumptions and objectives.

2. EQUATIONS

The governing equations employed in CFD are the mass conservation equation (also known as continuity equation), and Navier-stokes equation (also known as momentum equation).

2.1. Model assumptions

Some of the assumptions considered in setting up this model are:

1. the flow is not axisymmetrical.
2. the liquid phases are incompressible.
3. the pressure in the radial direction is constant.
4. the diameter of the pipe is sufficiently small compare with its length; the pipe is long enough for the flow to develop.
5. the effect of temperature is negligible

2.2. Governing equations

The equation for conservation of mass (or continuity equation) and momentum are given by Ansys Inc. [28] and Bird et al. [29]) as shown in equations (1) and (2), respectively. A momentum equation was used for the VOF. This depended on the volume fractions of all phases in the flow through density and viscosity parameters.

$$\frac{\partial}{\partial t} (\rho) + \nabla \cdot (\rho \vec{v}) = 0 \quad (1)$$

$$\frac{\partial}{\partial t} (\rho \vec{v}) + \nabla \cdot (\rho \vec{v} \vec{v}) = -\nabla P + \nabla \cdot [\mu (\nabla \vec{v} + \nabla \vec{v}^T)] + \rho \vec{g} + \vec{F} \quad (2)$$

Where \vec{F} is a body force, and μ is the viscosity of the phase. The tracking of the interface(s) between the phases is accomplished by the solution of a continuity equation for the volume fraction (α) of one (or more) of the phases. For the qth phase, equation (1) has the form of equation (3)

$$\frac{\partial \alpha_q}{\partial t} + \nabla \cdot (\alpha_q \vec{v}) = \frac{S \alpha_q}{\rho_q} \quad (3)$$

Where S is a source. The primary-phase volume fraction will be computed based on the constraint as shown on equation (4)

$$\sum_{q=1}^n \alpha_q = 1 \quad (4)$$

The geometric reconstruction scheme was used to calculate the fluxes at control volume faces required by the VOF model.

2.3. Turbulence models

Standard K-Epsilon Model

In order to simulate turbulence in this work, one of the popular RANS turbulent models, low-Reynolds-k-epsilon was used. The reason for this model is that it has demonstrated capability to properly simulate many industrial processes including multiphase flow. The model is described by the equations (5) to (8)

$$\frac{\partial}{\partial t} (\rho k) + \frac{\partial}{\partial x_j} (\rho k u_j) = \frac{\partial}{\partial x_j} \left[\left(\mu + \frac{\mu_t}{\sigma_k} \right) \frac{\partial k}{\partial x_j} \right] + P_k + P_b + \rho \epsilon - Y_M + S_k \quad (5)$$

$$\frac{\partial}{\partial t} (\rho \epsilon) + \frac{\partial}{\partial x_j} (\rho \epsilon u_j) = \frac{\partial}{\partial x_j} \left[\left(\mu + \frac{\mu_t}{\sigma_\epsilon} \right) \frac{\partial \epsilon}{\partial x_j} \right] - \rho C_{2\epsilon} \frac{\epsilon^2}{k} + C_{1\epsilon} \frac{\epsilon}{k} (P_k + C_{3\epsilon} P_b) + S_\epsilon \quad (6)$$

Where

$$\mu_t = \rho C_\mu \frac{k^2}{\epsilon} \quad (7)$$

$$C_{1\epsilon} = 1.44, \quad C_{2\epsilon} = 1.9, \quad \sigma_k = 1.0, \quad \sigma_\epsilon = 1.2 \quad C_\mu = 0.09 \quad (8)$$

2.4. Geometry and Mesh

In order to investigate the flow behavioural details observed in the experimental high viscosity oil-water flow rig, the rig is substituted and simplified by a 1-in horizontal pipe shown in Figure 1. The geometry is 3-Dimensional and its longitudinal cross section is illustrated in Figure 1. It is a 5m long, 1-in internal diameter horizontal pipe similar to the experimental arrangements. The pipe axis is always aligned with the z- axis and several measurements sections were placed along the pipe. The pre-validation was conducted using pressure drop data from experiment setup and empirical correlation of a single liquid phase of water and oil.



Figure 1: Longitudinal cross section of the mesh

The geometry and mesh that were used in this study were developed with Gambit 2.4 and imported into FLUENT 12.1 for the case simulations. The concentric inlet design was only considered in the CFD simulation to impose the water injection as shown in Figure 2 where water was injected in the annulus and oil injected at the centre.

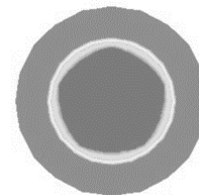


Figure 2: CFD annular flow inlet geometry description

The region near the wall was meshed finer than the rest of the cross section, as it contained greater amount of gradients. A mesh sensitivity analysis was conducted to identify the minimum mesh density that ensured that the solution was independent of the mesh size. The outcome over 30 seconds flow time is presented in Figure 3. The Eulerian-VOF CFD model which was used to study the flow of oil-water. The improvement introduced as User Defined Function (UDF) into the oil-water turbulence Low Reynolds k-epsilon (LRKE) model was also employed. The CFD results were validated using measurements of pressure gradient obtained from the experiments. Constant superficial velocities and atmospheric pressure were specified at the inlet and pressure outlet at the outlet boundaries of the CFD models. The temperature change along the channel was considered negligible. The relevant properties of the two fluids (oil and water) used in the simulation are as given in Table 1 while the mesh details for sensitivity analysis is on Table 2.

Table 1: Fluid properties

Fluid	Density @25°C (kg/m ³)	Viscosity @25°C (Pa.s)	Surface Tension @19°C (N/m)
Water	998.2	0.001003	0.026
Oil	916.2	3.149	0.026

Table 2: Mesh details for sensitivity analysis

Case	Domain	Structure	Nodes	No of cells
Mesh-1	3D	Hexahedral	75651	70000
Mesh-2	3D	Hexahedral	151151	140000
Mesh-3	3D	Hexahedral	251251	240000
Mesh-4	3D	Hexahedral	502251	480000
Mesh-5	3D	Hexahedral	1002501	960000

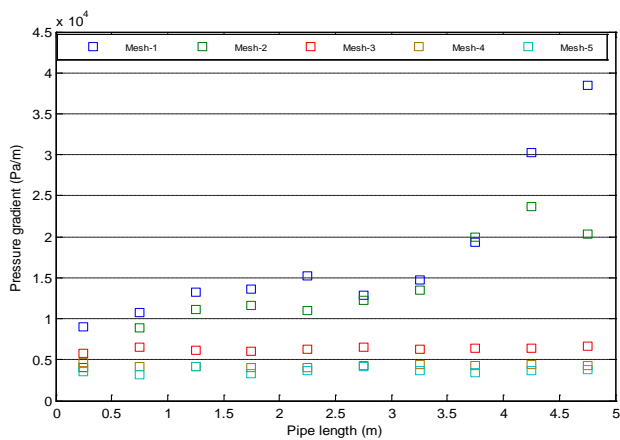


Figure 3: Pressure gradients of mesh profiles

2.5. Turbulence kinetic energy budget

The typical gradients of the turbulence models examined for the selection of a suitable model for the prediction of oil-water flow in horizontal pipe is as shown on Figure 4. This figure shows that the existing turbulence models are not capable of simulating oil-water pressure gradient in their present default state except they are improved or modified. It could be observed that the pressure gradient is on the increase with increase in the water superficial velocity; this presupposes that turbulence dictates the flow characteristics. Therefore if any of these turbulence models will give a better prediction of pressure gradient, an improvement of such is inevitable. Most of these models returned stratified flow pattern except for SKE turbulence models which gave annular flow of oil surrounded by water and also the presence of oil film on the pipe wall. Although SKE model presents good contour plot, this is not enough description of the flow behaviour as the pressure drop obtained does not compare well with the experimental result. Hence, there is need for inputs that influence these turbulence models to accommodate the impact of the second phase in this kind of flow. This section presents the attempt made in the present research to address this problem.

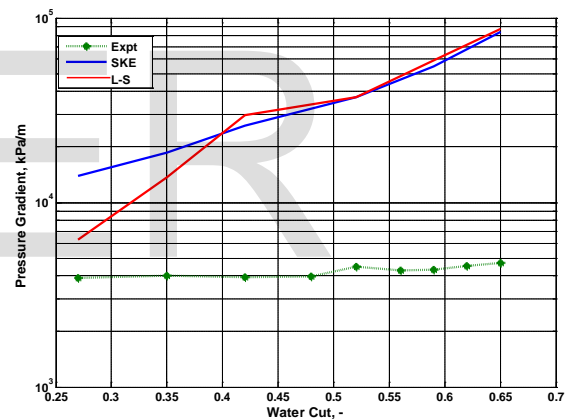


Figure 4: Comparison of default turbulence models results with experimental data of oil-water flow at 0.55m/s oil superficial velocity

The SKE model is widely used in industrial turbulent flow and heat transfer computation mainly due to its robustness, computational economy, and reasonable accuracy for a wide variety of turbulent flows. It is somewhat a semi-empirical model, mainly because the modelled transport equation for dissipation used in the model depends on phenomenological considerations and empiricism.

The modelled form of the dissipation equation used in the literature is a major weakness of the k-ε model as stated by Dewan [31]. This could be traced to the fact that the terms in the exact dissipation equation is modelled by few terms. Tennekes and Lumley [30] stated that the rate of change of $\frac{1}{2} \overline{u_i u_j}$ is due to transport by turbulent velocity fluctuation, pressure gradient work, transport by viscous stresses and two

kinds of deformation works. In other words, the modelling of the k and ϵ profiles is still the heart of $k - \epsilon$ model.

This development was based on the observation made on the behaviour of the pressure gradient profile, flow pattern and the fluctuating kinetic energy when the experimental data were compared with the simulation data, as shown in Figure 4 and Figure 5. It was observed in Figure 4 that irrespective of the damping functions from the existing models, the deviations of the pressure gradient were on the increase with the increase in the velocity of the secondary phase which is not the case in the obtained gradients from the experiments. Hence, the magnitude of the fluctuating energy predicted by the CFD and its dissipation was proposed to be contributing to the divergence of the gradient profile. Figure 5 reveals the uncorrelated feature of the energy fluctuations and their magnitudes when compared with those of the experiments. All of these observations and analyses led to a proposition to redefine the kinetic energy and its dissipation rate in order to suit this peculiar flow environment. This decision is in accordance to Tennekes and Lumley [30] assertion that turbulence behaviour and description depends on environment. Hence, the turbulence kinetic energy was assumed and proposed to behave linearly with respect to the velocity while its dissipation is assumed to have a quadratic behaviour as given in equations (8) to (10). In order to improve the turbulence effect in this unique high viscosity oil-water flow, four assumptions are proposed by the author to drive development:

1. the production of turbulent kinetic energy is not equal to its dissipation
2. the turbulent kinetic energy and its dissipation are dependent of the fractional constituents of the multi-phase flow,
3. turbulence behaviour is suppressed with increase in the superficial velocities of the phases because oil dispersion increases with increase in the superficial velocities of the phases, hence the mixing fluid becomes more viscous.
4. the turbulent kinetic energy is described as a linear function of the superficial velocities of the phases involve while its dissipation rate is defined as a quadratic function.

The correlations were developed by trial and error method using the qualitative analysis of Figure 5 whereby the fluctuating kinetic energy obtained from the experiments are compared with CFD's. It could be deduced that the fluctuations of flow in the CFD was about 5 to 8 order of magnitude different from that of the experiments. Figure 5 also reveals that the fluctuation in the experiments decreases with increase in water cut and vice versa in the CFD.

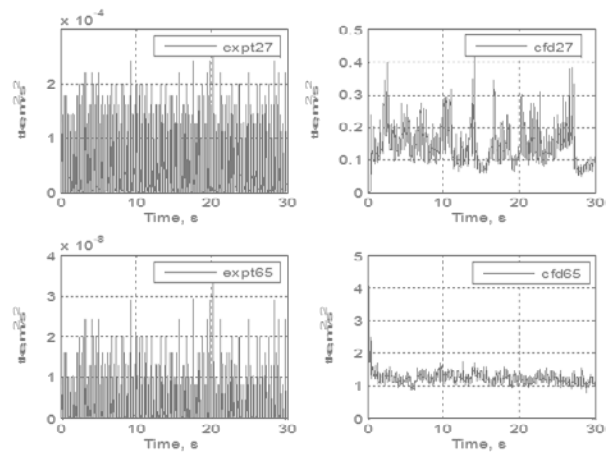


Figure 5: Comparison of fluctuation kinetic energy of experiment and CFD at 27% water cut

k and ϵ of the free stream can be estimated using empirical correlations gotten as functions of superficial velocities given as

$$k = Ax + B \tag{9}$$

and

$$\epsilon = Cx^2 + Dx + E \tag{10}$$

Where

$$x = \left(\frac{1}{\frac{V_{so}}{V_{sw}} + 1} \right) \tag{11}$$

Where

$$A = -0.2099 \text{ m}^2/\text{s}^2, \quad B = 0.1976 \text{ m}^2/\text{s}^2 \\ C = -221.88 \text{ m}^2/\text{s}^3, \quad D = 133.08 \text{ m}^2/\text{s}^3 \text{ and } E = 32.245 \text{ m}^2/\text{s}^3$$

These models were coded and hooked to FLUENT CFD solver as a user defined function for two-phase oil-water flow simulations.

2.6. Boundary Conditions

Appropriate and commonly encountered boundary conditions at the boundaries for computing the flow in a particular computational domain are employed in this research and stated below:

Inlet Provide distributions of k and ϵ along with flow properties, i.e., velocity and temperature, in the corresponding real situation. In some cases, it is difficult to obtain values of k and ϵ at the inlet and in such cases these can be obtained based on an approximation from the turbulent intensity T_i and a characteristic length L of the flow configuration is given as equation (12)

$$I = 0.07L \tag{12}$$

where I denotes a turbulent length scale and L characteristic length.

Outlet: At the outlet usually turbulence k and ϵ is taken equal to zero, the mean temperature (T_m) equal to the ambient temperature (T_1) and pressure (p) equal to the atmospheric pressure (p_1)

Wall: At the solid wall either the no slip condition using the low-Re version or wall function approach can be applied.

2.7. Solution Method

Finite Volume Method (FVM) discretisation scheme in Fluent 12.1 with an algebraic segregated solver and co-located grid arrangement was implemented to solve the system of partial and ordinary differential equations. In this grid arrangement pressure and velocity are both stored at cell centres. Versteeg and Malalasekera, [32] explain the details of the FVM discretisation. Since FLUENT uses a segregated solver, the continuity and momentum equations need to be linked, hence PISO algorithm which stands for Pressure Implicit with Splitting of Operators by Issa, [33] was employed because of its good performance to find a fast converged solution. PISO is a pressure-velocity calculation procedure that involves one predictor step and two corrector steps.

Flow regimes are known to be periodical in nature hence the unsteady solver was employed to simulate the flow behaviours. Since statistically steady-state of the flow behaviours are made up of several periodic flows the time employed to collect data in the experiments was adopted i.e. 30s. The variable time step method was adopted to prevent divergence and also to reduce the computation time of CPU. The time step was adjusted automatically based on the Courant number known as CFL after its authors (Courant-Friedrich-Lewy). The Courant number is a dimensionless number that compares the time step (Δt) in a calculation to the characteristic time of transit for a fluid element across a control volume. The global CFL condition is given by equation (13)

$$CFL_{global} = \Delta t_{global} * \max \left(\sum \frac{\text{outgoing fluxes}}{\text{volume}} \right) \quad (13)$$

where Δt_{global} is the global time step. The global Courant number employed in this research was 2 and the resulting time step varied from 1e-05 to 0.004s. Here a static contact angle ($\theta=90^\circ$) is applied for all simulation cases.

3. RESULTS AND DISCUSSION

The effect of mesh density on the pressure drop profile along the pipe is as shown on Figure 6. The mesh with 480,000 cells was considered suitable for simulation since the pressure drop difference from 960,000 cells is relatively 8%. This helped in saving the computational time. In the same vein, Figure 4 and Figure 5 informed the reliability of the model for the simulations because of their closeness in predicting the pressure drop profile of water and oil in the same flow channel. Figure 4 shows good match for water at high flow rate when compared with both Darcy-Weisbach (D-W) theoretical and experimental data, but under predicted the gradients at low flow rate. However, when it was used for high viscous oil, it was an excellent agreement with the D-W theoretical model while the experiment relatively reflected some deviations from the model (Figure 5). Generally, the CFD model possessed a good level of confidence for the subsequent simulations.

3.1. Pressure gradient

The results of both the CFD and experiments are compared in this section in order to make a better evaluation of the performance of the developed model. Figure 8 and Figure 9 compare the pressure gradients obtained from experiment with the results gotten from modified SKE and L-S, respectively for

3300cP oil at 0.55m/s. Figure 10 and Figure 11 are the comparisons obtained for 5000cP and 7500cP at 0.20m/s and 0.10m/s, respectively.

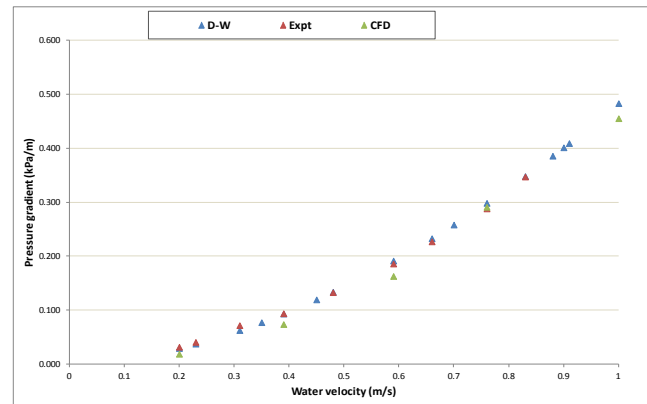


Figure 6: Comparison of D-W, Experimental and CFD pressure gradients of a single phase water in 1-in ID 5m long pipe

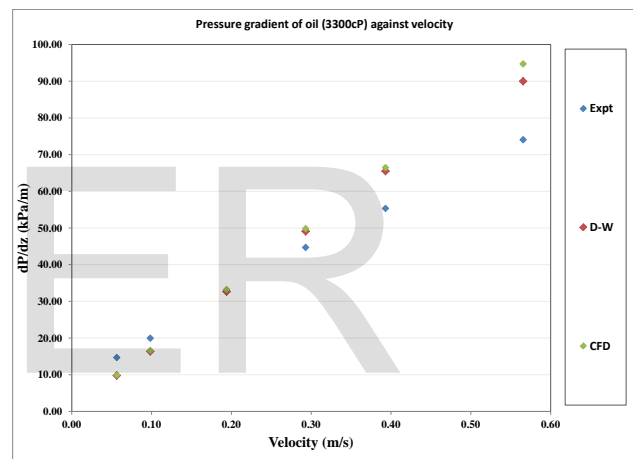


Figure 7: Comparison of CFD, D-W and Experimental pressure gradients of a single phase oil in 1-in ID 5m long pipe.

All of these plots are drawn from oil-water flow in horizontal pipe for varying water cut ranging from 0.0 – 1.0. Generally, it could be observed that the simulation results fairly compare with the experiments; Figure 8 shows that the popular SKE model in engineering field is still very suitable with a little modification, although most of the simulations were run with LRKE model. The choice was based on the fact that LRKE is known with capability to resolve the gradients close to the wall. In addition, Figure 8 shows a satisfactory comparison with the experiment except at 48 and 65 per cent water cut where CFD returned higher gradients; these could be due to the limitations in CFD or in the experimental data. At 65 per cent, perhaps the water which was the continuous phase due to its attributed turbulence caused an increased dispersion that transported bulk of the oil to the wall and hence increased the gradient. The deviations of the results in Figure 9 also could be discussed as the effect of mixing rules for the fluids' properties; at higher water cuts (i.e. greater than 48%), the model under predicted the experimental results while on few occasion at very low water cut, it is vice versa.

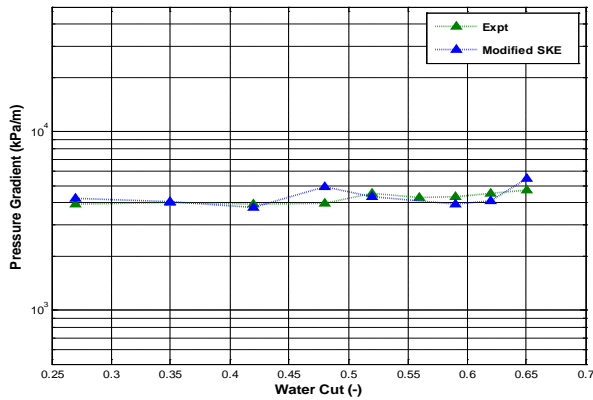


Figure 8: Pressure gradient against water cut @ $V_{so} = 0.55\text{m/s}$ for 3300cP oil using modified SKE CFD model

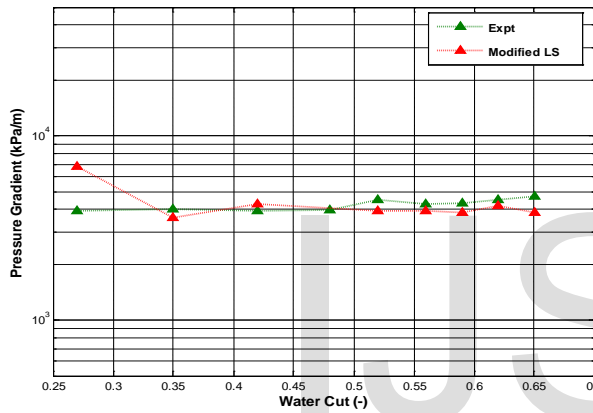


Figure 9: Pressure gradient against water cut @ $V_{so} = 0.55\text{m/s}$ for 3300cP oil using modified LRKE (L-S) CFD model

In Figure 10 and Figure 11, when the viscosity of oil was increased to 5000cP and 7500cP respectively, fairly good results were obtained but also with similar deviations of under predictions at very high water cut (say 75%) and vice versa at lower water cut. These deviations might be caused by numerical instability, since they are not present in all the cases simulated.

3.2. Flow regime identification

The flow regime identification studies are presented in this section using visualisation (i.e. subjective) and pressure signal trend and PDF analysis (i.e. objective) approaches. Samples of the observed oil-water flow configurations are presented to illustrate the flow patterns obtained in the course of the experiments. The flow pattern images are captured from side view of the pipe. Considering the flow contours obtained in this research, apart from Table 3 where oil is continuous and enveloped pockets of water, all the flow contours have oil film (fouling) on the pipe wall.

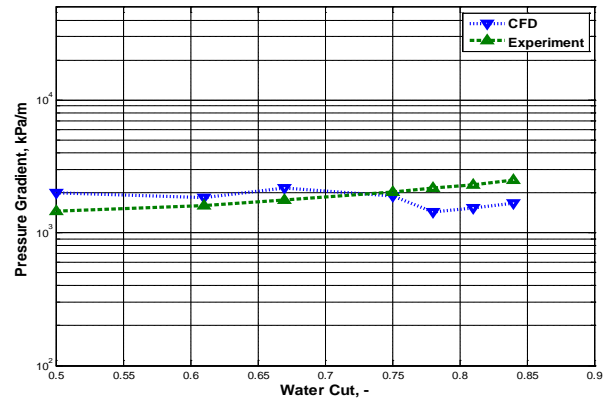


Figure 10: Pressure gradient against water cut @ $V_{so} = 0.20\text{m/s}$ for 5000cP oil using modified LRKE (L-S) CFD model

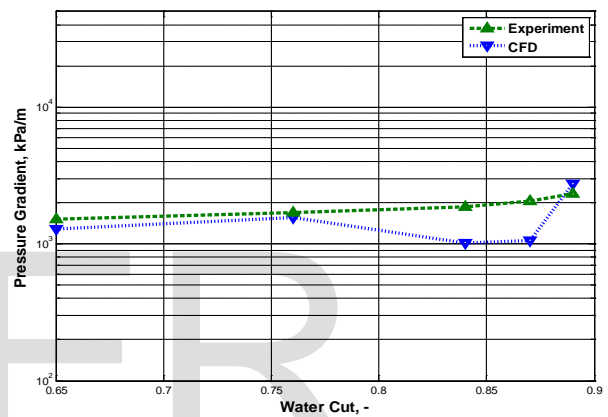


Figure 11: Pressure gradient against water cut @ $V_{so} = 0.10\text{m/s}$ for 7500cP oil using modified LRKE (L-S) CFD model

These are exact prediction of oil fouling observed in all the oil-water experimental campaigns. This was not captured by Kaushik et al. [13] in their research, perhaps their oil viscosity (0.22Pa.s) was too low or their mesh and/or models were not adequate.

In addition, it is important to mention that the CFD simulation in this research replicated all the flow patterns that were observed in the experiments. Table 3 presents a flow configuration labelled Water Plug in Oil (WPO) which was not visible to the camera but compared with the findings of McKibben et al. [34]. Table 4 compares well with the experiment at the same flow condition and labelled Oil Plug in Water (OPW/OF) as mentioned in the experiment. Water Assist Annular (WA-ANN) flow was presented as well in Table 5. It also compared favourably with the experiment. The Dispersed Oil in Water (DOW/OF) flow pattern in Table 6 was also predicted by the CFD.

Table 3: Contour-Experiment analysis of oil-water flow of 10000cP at $V_{so} = 0.11\text{m/s}$, and $V_{sw} = 0.02\text{m/s}$


Flow Condition	Water Plug in Oil (WPO)
Contour (a)	
Video (b)	Not visible because the water plug was covered by oil

Table 4: Contour-Experiment analysis of oil-water flow of 7500cP at $V_{so}=0.1\text{m/s}$ and $V_{sw}=0.8\text{m/s}$



Flow Condition	Oil Plug in Water (OPW/OF)
Contour (a)	
Video (b)	

Table 5: Contour-Experiment analysis of oil-water flow of 3300cP at $V_{so} = 0.55\text{m/s}$ and $V_{sw} = 1.0\text{m/s}$


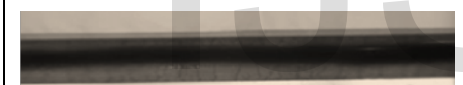


Flow Condition	Water Assist Annular Flow (ANN)
Contour (b)	
Video (c)	

Table 6: Contour-Experiment analysis of oil-water flow of 7500cP at $V_{so}=0.06\text{m/s}$ and $V_{sw}=0.80\text{m/s}$

Flow Condition	Dispersed Oil in Water (DOW)
Contour (b)	
Video (c)	

4. ACKNOWLEDGMENTS

The author would like to acknowledge the Petroleum Technology Development Programme (PTDF) of the Nigerian Government for their financial support on this project.

5. CONCLUSION

The superficial velocities of high viscosity oil and water strongly influenced both the pressure gradient and flow pattern of this multiphase flow. The flow pattern types were identified and reported from the visualisation (video) of the flow, description by the trend plot and PDF of the downstream pressure signals along with the statistical moments. The observed flow patterns are WPO, OPW/OF, WA-ANN, and

DOW/OF. The CFD simulation results are generally in agreement with the laboratory experimental results. This demonstrates the capabilities of CFD to model water assist flows observed in the experimental study of high viscosity oil-water flow. Good matches of pressure gradients and flow patterns between CFD and experiments were successfully obtained by imposing a concentric inlet condition at the inlet of the horizontal pipe coupled with a newly developed turbulent kinetic energy budget equation coded as user defined function which was hooked up to the turbulence models. These modifications aided satisfactory predictions.

ACKNOWLEDGMENT

The author would like to acknowledge the Petroleum Technology Development Programme (PTDF) of the Nigerian Government for their financial support on this project.

REFERENCES

- [1] Dusseault, M. (1993), "Cold Production and Enhanced Oil Recovery", Journal of Canadian Petroleum Technology, 32(9) : 28-38.
- [2] Dusseault, M., Geilikman, M. and Roggensack, W. (1995), "Practical requirements for sand production implementation in heavy oil applications", SPE International Heavy Oil Symposium. 19-21 June, Calgary, Alberta, Canada.
- [3] Besson, C. (2005), Resources to Reserves: Oil and Gas Technologies for the Energy Markets of the Future, OECD Publishing.
- [4] Owen, N. A., Inderwildi, O. R. and King, D. A. (2010), "The status of conventional world oil reserves – Hype or cause for concern?", Energy Policy, 38(8) :4743-4749.
- [5] Barnea, D., Shoham, O. and Taitel, Y. (1980), "Flow pattern characterization in two phase flow by electrical conductance probe", International Journal of Multiphase Flow, 6(5):387-397.
- [6] Martinez, A., Arirachakaran, S., Shoham, O. and Brill, J. (1988), "Prediction of Dispersion Viscosity of Oil/Water Mixture Flow in Horizontal Pipes", SPE Annual Technical Conference and Exhibition.
- [7] Brauner, N. and Moalem Maron, D. (1992), "Flow pattern transitions in two-phase liquid-liquid flow in horizontal tubes", International Journal of Multiphase Flow, 18(1): 123-140.
- [8] Trallero, J., Sarica, C. and Brill, J. (1997), "A study of oil-water flow patterns in horizontal pipes", Old Production & Facilities, 12(3) :165-172.
- [9] Angeli, P. and Hewitt, G. (2000), "Flow structure in horizontal oil-water flow", International Journal of Multiphase Flow, 26(7) :1117-1140.
- [10] Angeli, P. and Hewitt, G. (1999), "Pressure gradient in horizontal liquid-liquid flows", International Journal of Multiphase Flow, 24(7) :1183-1203.
- [11] Ooms, G. and Poesio, P. (2003), "Stationary core-annular flow through a horizontal pipe", Physical Review E, 68(6) :66301.
- [12] Rodriguez, O. M. H. and Bannwart, A. C. (2008), "Stability analysis of core-annular flow and neutral stability wave number", AIChE Journal, 54(1) :20-31.
- [13] Kaushik, V., Ghosh, S., Das, G. and Das, P. K. (2012), "CFD simulation of core annular flow through sudden contraction and expansion", Journal of Petroleum Science and Engineering, 86(1):153-164.
- [14] Bai, R., Chen, K. and Joseph, D. (1992), "Lubricated pipelining: stability of core-annular flow. Part 5: Experiments and comparison with theory". Journal. Fluid Mechanics.240 :97- 132
- [15] Kashid, M. N., Gerlach, I., Goetz, S., Franzke, J., Acker, J., Platte, F., Agar, D. and Turek, S. (2005), "Internal circulation within the liquid slugs of a liquid-liquid slug-flow capillary microreactor", Industrial & Engineering Chemistry

Research, 44(14) :5003-5010.

- [16] Kashid, M., Agar, D. and Turek, S. (2007), "CFD modelling of mass transfer with and without chemical reaction in the liquid-liquid slug flow microreactor", *Chemical Engineering Science*, 62(18):5102-5109.
- [17] Kashid, M., Rivas, D. F., Agar, D. and Turek, S. (2008), "On the hydrodynamics of liquid-liquid slug flow capillary microreactors", *Asia-Pacific Journal of Chemical Engineering*, 3(2) :151-160.
- [18] Kashid, M. N., Renken, A. and Kiwi-Minsker, L. (2010), "CFD modelling of liquid-liquid multiphase microstructured reactor: Slug flow generation", *Chemical Engineering Research and Design*, 88(3) :362-368.
- [19] Kashid, M., Kowalirski, W., Renken, A., Baldyga, J. and Kiwi-Minsker, L. (2012), "Analytical method to predict two-phase flow pattern in horizontal micro-capillaries", *Chemical Engineering Science*, 74:219-232.
- [20] Kashid, M., Kowalirski, W., Renken, A., Baldyga, J. and Kiwi-Minsker, L. (2012), "Analytical method to predict two-phase flow pattern in horizontal micro-capillaries", *Chemical Engineering Science*, 74:219-232.
- [21] Ghosh, S., Das, G. and Das, P. K. (2010), "Simulation of core annular down-flow through CFD-A comprehensive study", *Chemical Engineering and Processing: Process Intensification*.
- [22] Sotgia, G., Tartarini, P. and Stalio, E. (2008), "Experimental analysis of flow regimes and pressure drop reduction in oil-water mixtures", *International Journal of Multiphase Flow*, 34(12):1161-1174.
- [23] Prada, J. W. V. and Bannwart, A. C. (2001c), "Modeling of vertical core-annular flows and application to heavy oil production", *Journal of energy resources technology*, 123 : 194.
- [24] Bensakhria, A., Peysson, Y. and Antonini, G. (2004a), "Experimental study of the pipeline lubrication for heavy oil transport: Pipeline transportation of heavy oils= Ecoulement des bruts lourds dans les conduits", *Oil & gas science and technology*, 59(5) :523-533.
- [25] Balakhrisna, T., Ghosh, S., Das, G. and Das, P. (2010b), "Oil-water flows through sudden contraction and expansion in a horizontal pipe-Phase distribution and pressure drop", *International Journal of Multiphase Flow*, 36(1) :13-24.
- [26] Strazza, D., Grassi, B., Demori, M., Ferrari, V. and Poesio, P. (2011), "Core-annular flow in horizontal and slightly inclined pipes: Existence, pressure drops, and hold-up", *Chemical Engineering Science*. 66(12) : 2853-2863
- [27] Abdullah, A. (2011), "Quantifying guidelines and criteria for using turbulence models in complex flows", PhD Thesis, Cranfield University.
- [28] Ansys Inc., (2003), "Fluent user's guide", Ansys Inc., 2: 3.
- [29] Bird, R. B., Stewart, W. E. and Lightfoot, E. N. (2006), *Transport phenomena*, Wiley.
- [30] Tennekes, H. and Lumley, J. L. (1972) *A first course in turbulence*, MIT press. UK.
- [31] Dewan, A. (2010), *Tackling Turbulent Flows in Engineering*, Springer-Verlag Berlin Heidelberg.
- [32] Fersteg, H. K. and Malalasekera, W. (2007) *An Introduction to Computational Fluid Dynamics: the Finite Volume Method*, Prentice Hall.
- [33] Issa, R. (1986), "Solution of the implicitly discretised fluid flow equations by operator-splitting", *Journal of Computational physics*, 62(1): 40-65.
- [34] McKibben, M. J., Gillies, R. G. and Shook, C. A. (2000), "A laboratory investigation of horizontal well heavy oil-water flows", *The Canadian Journal of Chemical Engineering*, 78(4):743-751.